Atomic Force Microscopy Imaging of Crystalline Sucrose in Alcohols

Teduka, Yuya
Sasahara, Akira
Onishi, Hiroshi

(Citation)
ACS Omega,5(6):2569-2574

(Issue Date)
2020-02-18

(Resource Type)
journal article

(Version)
Version of Record

(URL)
https://hdl.handle.net/20.500.14094/90007021

ACS OMEGA

http://pubs.acs.org/journal/acsodf

Article

Atomic Force Microscopy Imaging of Crystalline Sucrose in Alcohols

Yuya Teduka, Akira Sasahara, and Hiroshi Onishi*

Cite This: *ACS Omega* 2020, 5, 2569−2574

Read Online

ACCESS | Metrics & More | Article Recommendations | Supporting Information

ABSTRACT: Imaging nanometer- or molecule-scale topography has been achieved by dynamic atomic force microscopy (AFM) when a solid object of interest is damaged by vacuum exposure or electron irradiation. Imaging in a liquid offers a means to remove contaminations from the surface scanned using the microscope tip when the object is soluble to the surrounding liquid, typically water. In the present study, we attempted to take topographic images of crystalline sucrose. A problem arose due to the high solubility of this compound to water. Cantilever oscillation could not be excited in the saturated, viscous aqueous solution. By using *n*-hexanol instead of water, the solubility in the solvent and thus viscosity of the solution were reduced sufficiently to excite cantilever oscillation. Single-height steps and sucrose molecules were recognized in the images and thereby recorded on the (001)-oriented facets of sucrose crystals. Furthermore, two-dimensional distribution of liquid-induced force pushing or pulling the tip was mapped on planes perpendicular to the hexanol−sucrose interface. Observed uneven force distributions indicated liquid hexanol structured on the corrugated surface of sucrose. The viscosity tuning demonstrated here, which is not limited to hexanol instead of water, extends the range of liquid−solid interfaces to be probed by dynamic AFM.

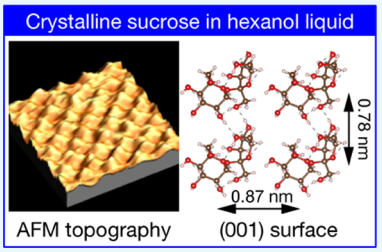

1. INTRODUCTION

Structure determination of solid surfaces is a fundamental task in chemistry and physics at interfaces. Electron microscopy provides a vital tool to visualize nanometer- and atom-scale architectures of materials. Low-energy electron diffraction is feasible to determine surface atom coordinates. However, organic compounds are easily damaged by exposing them to a vacuum or irradiating them with electrons. Crystal truncation rod analysis of X-ray diffraction offers a structure determination free from electron irradiation,[1] although a synchrotron facility is required to provide X-rays of sufficient intensity. In laboratories, atomic force microscopy (AFM) is used for visualizing nanometer-scale and even molecule-scale topography of organic materials.

It is required in AFM imaging to maintain an object of interest with no contamination beneath the scanning tip. Immersion in a liquid is a way to shield the object from the air, the major source of possible contaminations. The imaging liquid plays a further role when the object is soluble to the liquid. Even if the surface is contaminated prior to immersion, the contaminated layers are spontaneously removed. By applying this simple and efficient means, molecule- or atom-scale imaging of 4-nitroaniline,[2,3] $CaCO_3$,[4−10] $MgCO_3$,[11] and alkali halides[12−14] has been achieved in aqueous solutions. Crystalline rubrene has also been imaged in an ionic liquid.[15] In the present study, we apply this method to image crystalline sucrose ($C_{12}H_{22}O_{11}$). A problem arises due to its high solubility in water, 67 wt % at 293 K.[16] Cantilever oscillation cannot be excited in the saturated, viscous solution of sucrose. In unsaturated solutions, sucrose crystals rapidly dissolve, which makes imaging scans difficult. By using aliphatic alcohols (*n*-hexanol, *n*-butanol, and *n*-octanol) instead of water, the solubility and viscosity of the liquid are reduced to achieve imaging with a molecule-scale resolution. Two-dimensional distribution of liquid-induced force pushing or pulling the tip has been further mapped on planes perpendicular to the hexanol−sucrose interface. Observed uneven force distributions evidenced liquid hexanol structured on the corrugated surface of sucrose. The imaging liquid should be less viscous than water when saturated with sucrose, harmless to an operator since our liquid cell is open to the laboratory air, and inert on metals and adhesives of the cantilever assembly. The alcohols satisfy these requirements.

2. EXPERIMENTAL SECTION

2.1. Sucrose Crystals. A saturated aqueous solution of sucrose (Wako, guaranteed reagent) was prepared at 350 K and cooled to room temperature. Centimeter-sized crystals terminated with smooth facets appeared in the cooled solution, as shown in Figure S1 in the Supporting Information. The crystallographic indices of major facets were identified to be (001), (101), or (011) by comparing the crystal shapes to those reported in an earlier study.[17] The authors focused on the (001) facets, which were the most developed and hence had the most stable truncation on crystalline sucrose. Facets of this orientation were identified by visual inspection and then

Received: August 18, 2019
Accepted: January 24, 2020
Published: February 4, 2020

https://dx.doi.org/10.1021/acsomega.9b02660
ACS Omega 2020, 5, 2569−2574

checked by X-ray diffraction. Peaks assignable to (001), (002), and (003) diffraction were recognized, as shown in Figure S2, to evidence the proper orientation of the visually identified facets. The (001) plane distance was deduced to 1.06 nm, in accordance with the reported length. A wafer exposing two (001) facets at the top and bottom was prepared by cleaving a crystal using a scalpel and set on a fluorocarbon polymer plate designed for AFM imaging in a liquid.[18]

2.2. AFM Imaging. An SPM-8100FM (Shimadzu) microscope in development was operated at room temperature (RT). A droplet of the imaging liquid, *n*-hexanol (Wako, 97.0+%), was placed on a cleaved sucrose wafer, and the cantilever assembly was placed on the top. A piezo actuator oscillated a silicon cantilever (BudgetSensors, Tap300Al-G). The typical spectrum of thermally excited cantilever oscillation is shown in Figure 1. The quality factor of oscillation resonance was

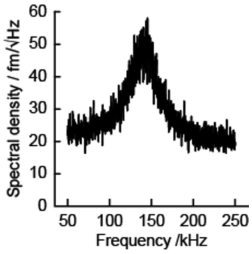

Figure 1. Typical spectrum of thermally excited cantilever oscillation in *n*-hexanol.

deduced to 3.4 by fitting the spectrum with the nominal spring constant of the cantilevers, 40 N m^{-1}. Figure S3 shows the oscillation spectra in *n*-butanol (Wako, 99.0+%) and *n*-octanol (Wako, 98.0+%) with quality factors of 3.9 and 2.6 in butanol and octanol, respectively. One common cantilever was used while observing the three spectra shown in Figure 1 and Figure S3.

Let the authors note the efficiency of cantilever excitation in pure hexanol. The excitation voltage applied on the piezo actuator was larger by 2.4 times than that required in pure water to yield common amplitude of resonance oscillation, since the viscous response of the liquids determined the excitation efficiency. In pure water, the quality factor of oscillation resonance increased to 10. Hexanol, which is more viscous than water, required larger amplitude of excitation and led to a smaller quality factor. High-resolution imaging was still possible in the circumstances, as will be described in the following section. The viscosity of hexanol should be insensitive to the presence of sucrose crystals in it. The solubility of sucrose in hexanol was so low that the dissolution could not be visually recognized.

The piezoelectric scanner of the microscope was calibrated in lateral coordinates by scanning a muscovite mica wafer in aqueous KCl solution (0.1 mol l^{-1}). A hexagonal structure with a repetition length of 0.52 nm on mica was reproduced in the observed topography with errors of 10% or less. The vertical coordinate was checked with step heights on $CaCO_3$ (104) wafers. Another microscope (SPM-9700, Shimadzu) was operated with silicon cantilevers (Nanosensors, PPP-NCHAuD) for imaging sucrose wafers in the air. Images observed with the two microscopes were analyzed with WSxM software.[19] The molecule assembly of sucrose crystals was graphically presented in this paper using the VESTA program.[20]

3. RESULTS AND DISCUSSION

3.1. Sucrose Dissolution in Hexanol. Terraces and steps were recognized on the cleaved (001) surfaces. Figure 2a

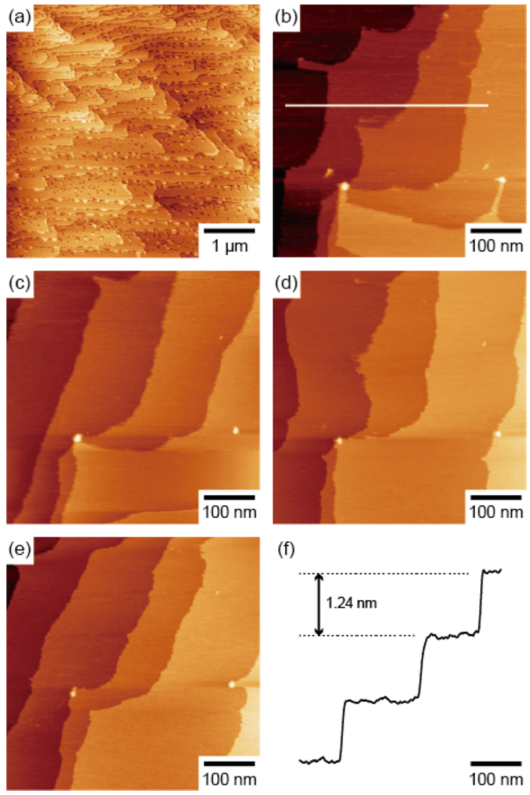

Figure 2. Terraces and steps on the cleaved sucrose (001) surfaces. (a) Topographic image scanned in the air. Image size, 5 μm square. Cantilever excitation frequency, 281 kHz. Another cleaved wafer scanned in hexanol. (b–e) Four consecutively observed images. Image size, 500 nm square. Frequency-shift (Δf) set point, +36 Hz. Peak-to-peak amplitude of cantilever oscillation (A), 0.87 nm. (f) Cross section determined along the inserted line in panel b.

shows the topographic image observed in the air in the amplitude-modulation mode. In this mode of imaging, the cantilever was oscillated at a fixed frequency with constant excitation amplitude from the piezo actuator. The vertical tip position was feedback-regulated to maintain the oscillation amplitude at the free end of the cantilever constant. Round-shaped holes with diameters of 50–100 nm were present over terraces with widths of 0.5–1 μm. The terraces and steps gradually collapsed in the air probably by absorbing moisture.

Another cleaved wafer was immersed in pristine hexanol and imaged in the frequency-modulation mode. In this mode, the cantilever was always resonantly oscillating with a constant oscillation amplitude at the free end (A). The vertical tip position was regulated to maintain the shift of resonance frequency (Δf) constant. A positive Δf indicated repulsive tip–surface force. Four topographic images consecutively observed at intervals of 10 min are shown in panels b–e of Figure 2. Two small particles, probably insoluble contaminants, created marks on the surface. Terraces that are 100–300 nm wide appeared with no round-shaped pits. The terraces receded from left to right during 40 min of imaging. The receding terraces indicated a low but finite sucrose solubility in hexanol and made the sucrose surface clean spontaneously as desired.

https://dx.doi.org/10.1021/acsomega.9b02660
ACS Omega 2020, 5, 2569–2574

The receding terraces were separated by regular-height steps. A cross section determined along the line in panel b showed a regular step height of 1.24 nm. The step height determined in the AFM topography agrees with an accuracy of 14% with the unit cell length along the [001] axis of crystalline sucrose, which was reported to be 1.09 nm in an earlier study[21] and confirmed in our X-ray diffraction analysis. The deviations can be ascribed to incomplete calibration of the z coordinate of the scanner.

One unit cell contains two molecule layers perpendicular to the [001] axis, as illustrated in Figure 3a. Adjacent layers are

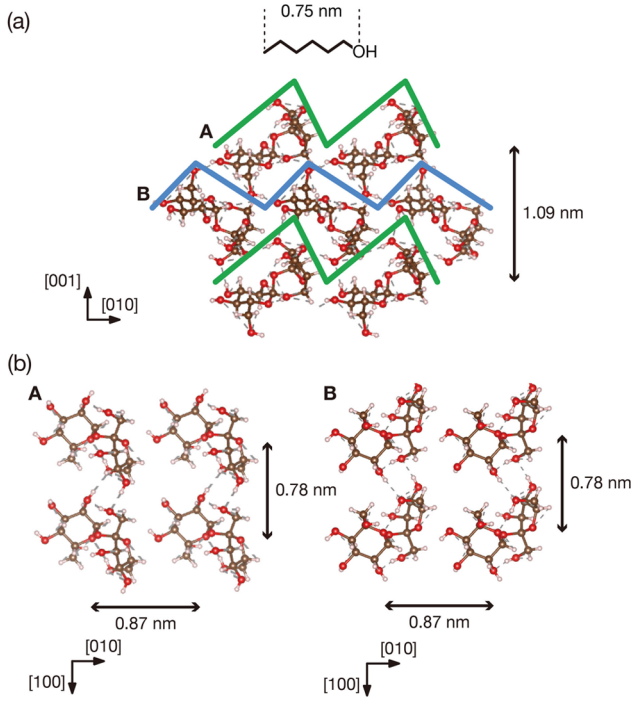

Figure 3. Two possible terminations on the sucrose (001) surface. (a) Side and (b) top views with brown, red, and white spheres representing carbon, oxygen, and hydrogen atoms, respectively. An *n*-hexanol molecule in the all-trans conformation is depicted in panel a to show its scale.

separated by nearly a half of the unit cell length. The observed step height regulated to be the unit cell length indicated that one of the two terminations, A or B, is more stable in hexanol than the other. Figure 3b shows the top view of the two terminations with the six-membered ring lying parallel to the surface and the five-membered ring nearly perpendicular. Sucrose molecules are hydrogen-bonded with each other in crystals. Four hydrogen bonds per molecule should break on the heavily corrugated termination A. The weakly corrugated termination B with two broken hydrogen bonds should be more stable than termination A.

3.2. Topographic Imaging with a Molecular Resolution. To resolve the fine features, we magnified one of the terraces and increased the frequency-shift set point. The increased set point required an increased tip−surface repulsive force during the feedback regulation, leading to a reduced tip−surface distance. Figure 4a presents the molecule-sized features recognized in the raw image thereby obtained. Two-dimensionally ordered protrusions were recognized with vertical corrugations of 0.03−0.04 nm, as shown in the cross sections in panels b and c. The size of the two-dimensional unit cell was

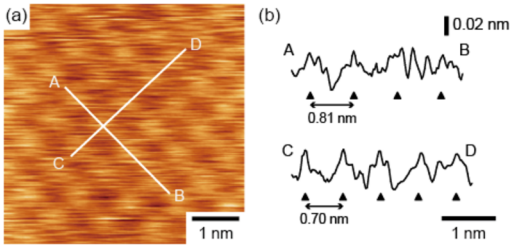

Figure 4. Sucrose molecules on the (001) terrace. (a) Raw topographic image observed in hexanol. Image size, 5 nm square. Δf, +231 Hz. A, 0.33 nm. (b) Cross sections determined along A−B and C−D lines and then smoothed.

0.78 nm × 0.86 nm with corner angles of 90°. The length and angle of the unit cell vectors agreed with those in theory, which are given in Figure 3b. The protrusions are therefore assigned to individual sucrose molecules exposed on the surface. In AFM imaging of molecule-sized features, the scanned object sometimes drifts relative to the tip due to thermal expansion. Leaving the microscope is an effective way to reduce drifts. Since our imaging liquid was exposed to air, the low vapor pressure of hexanol (0.06 kPa at 293 K)[22] helped us to continuously scan a sucrose wafer for more than 5 h. The unit cell dimensions were determined free from drift corrections.

Water molecules adsorbed strongly on mica and $CaCO_3$[7] to be recognized as atomic-scale protrusions in topography determined with FM-AFM. Their adsorption sites are metal cations exposed on the surface. Hexanol or water adsorbed on sucrose, if any, should be bound through hydrogen bonds. It is less probable that the hydrogen-bonded molecules were solidified as water on the metal-containing compounds.

Imaging in *n*-butanol and *n*-octanol was further examined to test the feasibility of alcohols with short or long alkyl chains. Typical images are shown in Figure S4. They are qualitatively similar to the image shown in Figure 4. Butanol presented a slightly better signal-to-noise ratio probably due to its lower viscosity; whereas, the vapor pressure of this liquid (0.6 kPa at RT)[22] is higher by one order of magnitude than that of hexanol, and it has limited feasibility for continuous scans. Octanol was more viscous than the other two alcohols and showed a reduced quality factor of cantilever oscillation. *n*-Hexanol was hence the most feasible liquid among the three alcohols examined.

3.3. Hexanol Liquid Structured on the Sucrose Surface. Atomic force microscopy operating in the frequency-modulation mode provides a tool for detecting uneven density distribution of liquids. The homogeneous density distribution of hexanol liquid is modified by exposing it to the sucrose surface. Figure 5a shows the cross-sectional Δf map observed on a plane perpendicular to the sucrose surface. The oscillating cantilever was scanned vertically from the bulk hexanol to the surface. The frequency shift was simultaneously recorded as a function of the vertical coordinate to obtain one Δf−distance curve at one lateral position. The vertical scans were aborted when Δf reached a predetermined threshold, +700 Hz when acquiring the map shown in Figure 5a, to prevent severe contact with the surface. By repeating 256 vertical scans along the lateral coordinate parallel to the [010] direction, the Δf map of the plane perpendicular to the surface was constructed.

The observed Δf map is regarded as an approximate force distribution on the plane. A repulsive tip−surface force causes

https://dx.doi.org/10.1021/acsomega.9b02660
ACS Omega 2020, 5, 2569−2574

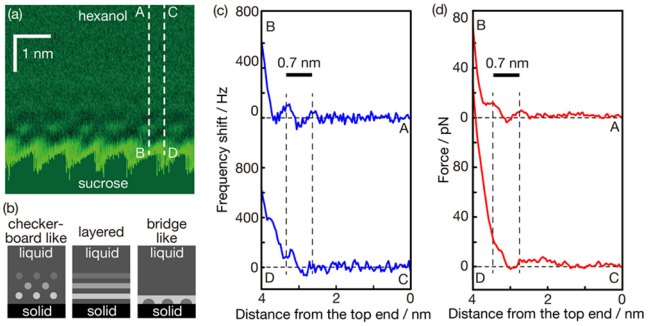

Figure 5. Hexanol liquid over sucrose (001). Cross-sectional Δf distribution determined on the plane perpendicular to the surface and parallel to the [010] direction with 256 vertical scans. (a) Picture of the aspect ratio of the lateral and vertical scales tuned to be unity. A positive (or negative) Δf with a bright (or dark) color. (b) Checker-board-like, layered, and bridge-like Δf maps reported in earlier studies. (c) Δf–distance curves obtained on the A–B and C–D lines. (d) Force–distance curves converted from the Δf–distance curves. *A*, 0.09 nm.

a positive frequency shift, while the relation between the force and Δf is nonlinear.[23] The brightest region at the bottom distribution represents the boundary of liquid hexanol and crystalline sucrose. When the tip reached that region, the repulsive force increased monotonically. This is a sign of contact of the tip on the solid. The envelope of the brightest region periodically corrugated along the lateral coordinate to produce a saw-tooth-like wave. Maxima and minima of the wave appeared alternately with a repetition length of 0.81 nm, reproducing the periodic length observed in the topographic image (0.86 nm).

The amplitude of the saw-tooth corrugation (Figure 5) was greater than that determined in the topographic image (Figure 4). In the Δf mapping, the cantilever approached the surface until Δf achieved +700 Hz with an oscillation amplitude of 0.09 nm. The topographic image shown in Figure 4 was determined with a Δf set point of +231 Hz and cantilever oscillation amplitude of 0.33 nm. Though the oscillation amplitudes were different, the authors expected that the tip was further pushed into the interface in the Δf mapping than in the topographic imaging. The saw-tooth corrugation reconstructed in the Δf map (Figure 5) should hence present a more precise trace of sucrose topography. Tip indentation in the sucrose surface was excluded since scratched features, as a sign of indentation, have not been observed in consecutive scans.

In liquid hexanol, bright and dark patches were laterally and vertically ordered to produce a checker-board-like pattern, as illustrated in the left panel of Figure 5b. The checker-board-like pattern decayed in intensity with increasing the distance from the surface to present two or possibly three layers of bright patches. The lateral repetition length in the patterned distribution matched the saw-tooth-like topography of the surface. The identical repetition lengths indicate that the physical corrugation and/or chemical composition on the surface induced the uneven density distribution of hexanol liquid.

The quantitative relation between the tip–surface force and the local liquid density is not direct, though a simple scheme for interpretation (solvent tip approximation) has been proposed.[24,25] Here, the comparison of the Δf map at the hexanol–sucrose (001) interface with the Δf maps observed on other liquid–solid interfaces has been made in a qualitative manner. Smooth liquid layers were formed on atomically flat surfaces of graphite[26−29] and the CH_3-terminated thiolate monolayer,[30] as depicted in the middle panel of Figure 5b. Bridge-like forms of the first water layer (the right panel of Figure 5b) were reported on flat and hydrophilic materials, mica,[31,32] and OH- and COOH-terminated thiolate monolayers.[33] Those features are different from the lateral and vertical ordering of bright and dark patches observed in the present study. Patches ordered in a similar symmetry have been found in water on 4-nitroaniline,[2,3] $CaCO_3$,[4−10] $MgCO_3$,[11] KBr,[13] and NaCl.[14] A common characteristic of these solids including sucrose (001) is the physical corrugation on their surfaces when compared with graphite, mica, and the thiolate monolayers. 4-Nitroaniline presented a rough surface topography according to the orientation of the surface molecules. The alkaline-earth metal carbonates also provided corrugated topography with carbonate anions protruding from the cleaved surface. The alkali metal cations and halogen anions created physical corrugations on the alkali metal–halide surfaces. We therefore suppose that physical corrugations, represented by the saw-tooth-like envelope (Figure 5), played a major role in structuring hexanol on sucrose (001).

Typical Δf–distance curves are depicted in Figure 5c. Four curves neighboring along the vertical lines A–B or C–D in panel a were picked up and averaged to make the curves in panel c. The averaged Δf–distance curves were then converted to force–distance curves shown in panel d, following Sader and Jarvis.[23] Two force maxima and two or three minima were recognized in curve A–B, in addition to the monotonic increase caused by the partial tip contact to the surface. The two maxima were separated by 0.7 nm, and the separation length should correspond to the distance of two neighboring liquid layers. When liquid alkanes[30] and oxygenated alkanes[28,29] are placed on flat surfaces, smoothly layered structures were produced with a layer-to-layer distance of 0.6 nm. This distance has been interpreted with the thickness of these chain-formed compounds statistically in the all-trans conformation. The distance observed in the present study is close to this length. On the other hand, the distance from the oxygen atom to the carbon atom at the other end is 0.75 nm along the molecular axis of all-trans hexanol, as depicted in Figure 3a. Standing orientation with some inclination cannot be ruled out. Hydrogen bonding with OH groups exposed on the sucrose surface would make alcohol molecules stand up.

4. CONCLUSIONS

A sucrose (001) surface was cleaved in the air and imaged with frequency-modulation AFM in *n*-hexanol, *n*-butanol, and *n*-octanol. The finite and limited solubility of sucrose in the short-chain alcohols played a triple role in imaging; the moisture-sensitive surface was shielded from the air. Possible contaminations were spontaneously lifted off. Cantilever oscillation was excited in the less viscous solution even saturated with sucrose. Terraces separated by regular-height steps were thereby imaged in hexanol. The regulated step height, 1.2 nm, suggested that one of the two possible terminations of normal to the [001] axis is stable. Sucrose molecules were recognized on the terraces with no sign of surface reconstruction. The two-dimensional force distribution was observed on planes perpendicular to the hexanol–sucrose interface to show liquid hexanol structured on the physically corrugated sucrose surfaces. The choice of imaging liquids demonstrated here, which should not be limited to one

https://dx.doi.org/10.1021/acsomega.9b02660
ACS Omega 2020, 5, 2569−2574

particular solvent, helps to conduct high-resolution imaging of other readily soluble materials.

■ ASSOCIATED CONTENT

Supporting Information

The Supporting Information is available free of charge at https://pubs.acs.org/doi/10.1021/acsomega.9b02660.

Sucrose crystal shape and XRD and AFM results (PDF)

■ AUTHOR INFORMATION

Corresponding Author

Hiroshi Onishi − *Department of Chemistry, School of Science, Kobe University, Kobe 657-8501, Japan;* orcid.org/0000-0003-1873-9105; Email: oni@kobe-u.ac.jp

Authors

Yuya Teduka − *Department of Chemistry, School of Science, Kobe University, Kobe 657-8501, Japan*

Akira Sasahara − *Department of Chemistry, School of Science, Kobe University, Kobe 657-8501, Japan*

Complete contact information is available at: https://pubs.acs.org/10.1021/acsomega.9b02660

Notes

The authors declare no competing financial interest.

■ ACKNOWLEDGMENTS

Tomoya Fujiwara of Kobe University assisted Y.T. in observing X-ray diffraction. Dr. Masato Hirade and Shiho Moriguchi of Shimadzu Corporation helped A.S. in determining cantilever oscillation spectra. This work was supported by the JSPS KAKENHI (grant no. JP18K19058) and Special Coordination Funds for Promoting Science and Technology, Creation of Innovation Centers for Advanced Interdisciplinary Research Areas (Innovative Bioproduction, Kobe).

■ REFERENCES

(1) Wakabayashi, Y.; Takeya, J.; Kimura, T. Sub-Å Resolution Electron Density Analysis of the Surface of Organic Rubrene Crystals. *Phys. Rev. Lett.* **2010**, *104*, No. 066103.

(2) Nishioka, R.; Hiasa, T.; Kimura, K.; Onishi, H. Specific Hydration on *p*-Nitroaniline Crystal Studied by Atomic Force Microscopy. *J. Phys. Chem. C* **2013**, *117*, 2939−2943.

(3) Spijker, P.; Hiasa, T.; Musso, T.; Nishioka, R.; Onishi, H.; Foster, A. S. Understanding the Interface of Liquids with an Organic Crystal Surface from Atomistic Simulations and AFM Experiments. *J. Phys. Chem. C* **2014**, *118*, 2058−2066.

(4) Imada, H.; Kimura, K.; Onishi, H. Water and 2-Propanol Structured on Calcite (104) Probed by Frequency-Modulation Atomic Force Microscopy. *Langmuir* **2013**, *29*, 10744−10751.

(5) Araki, Y.; Tsukamoto, K.; Takagi, R.; Miyashita, T.; Oyabu, N.; Kobayashi, K.; Yamada, H. Direct Observation of the Influence of Additives on Calcite Hydration by Frequency Modulation Atomic Force Microscopy. *Cryst. Growth Des.* **2014**, *14*, 6254−6260.

(6) Wastl, D. S.; Judmann, M.; Weymouth, A. J.; Giessibl, F. J. Atomic Resolution of Calcium and Oxygen Sublattices of Calcite in Ambient Conditions by Atomic Force Microscopy Using qPlus Sensors with Sapphire Tips. *ACS Nano* **2015**, *9*, 3858−3865.

(7) Fukuma, T.; Reischl, B.; Kobayashi, N.; Spijker, P.; Canova, F. F.; Miyazawa, K.; Foster, A. S. Mechanism of atomic force microscopy imaging of three-dimensional hydration structures at a solid-liquid interface. *Phys. Rev. B* **2015**, *92*, 155412.

(8) Söngen, H.; Nalbach, M.; Adam, H.; Kühnle, A. Three-dimensional atomic force microscopy mapping at the solid-liquid interface with fast and flexible data acquisition. *Rev. Sci. Instrum.* **2016**, *87*, No. 063704.

(9) Miyata, K.; Tracey, J.; Miyazawa, K.; Haapasilta, V.; Spijker, P.; Kawagoe, Y.; Foster, A. S.; Tsukamoto, K.; Fukuma, T. Dissolution Processes at Step Edges of Calcite in Water Investigated by High-Speed Frequency Modulation Atomic Force Microscopy and Simulation. *Nano Lett.* **2017**, *17*, 4083−4089.

(10) Tracey, J.; Miyazawa, K.; Spijker, P.; Miyata, K.; Reischl, B.; Canova, F. F.; Rohl, A. L.; Fukuma, T.; Foster, A. S. Understanding 2D atomic resolution imaging of the calcite surface in water by frequency modulation atomic force microscopy. *Nanotechnology* **2016**, *27*, 415709.

(11) Söngen, H.; Marutschke, C.; Spijker, P.; Holmgren, E.; Hermes, I.; Bechstein, R.; Klassen, S.; Tracey, J.; Foster, A. S.; Kühnle, A. Chemical Identification at the Solid-Liquid Interface. *Langmuir* **2016**, *33*, 125−129.

(12) Ichii, T.; Negami, M.; Sugimura, H. Atomic-Resolution Imaging on Alkali Halide Surfaces in Viscous Ionic Liquid Using Frequency Modulation Atomic Force Microscopy. *J. Phys. Chem. C* **2014**, *118*, 26803−26807.

(13) Arai, T.; Koshioka, M.; Abe, K.; Tomitori, M.; Kokawa, R.; Ohta, M.; Yamada, H.; Kobayashi, K.; Oyabu, N. Atom-Resolved Analysis of an Ionic KBr(001) Crystal Surface Covered with a Thin Water Layer by Frequency Modulation Atomic Force Microscopy. *Langmuir* **2015**, *31*, 3876−3883.

(14) Ito, F.; Kobayashi, K.; Spijker, P.; Zivanovic, L.; Umeda, K.; Nurmi, T.; Holmberg, N.; Laasonen, K.; Foster, A. S.; Yamada, H. Molecular Resolution of the Water Interface at an Alkali Halide with Terraces and Steps. *J. Phys. Chem. C* **2016**, *120*, 19714−19722.

(15) Yokota, Y.; Hara, H.; Morino, Y.; Bando, K.; Imanishi, A.; Uemura, T.; Takeya, J.; Fukui, K. Molecularly clean ionic liquid/rubrene single-crystal interfaces revealed by frequency modulation atomic force microscopy. *Phys. Chem. Chem. Phys.* **2015**, *17*, 6794−6800.

(16) In *CRC Handbook of Chemistry and Physics*; 92nd ed.; Haynes, W. M., Lide, D. R., Eds.; CRC Press: Boca Raton, FL, 2011; pp 5−185.

(17) Saska, M.; Myerson, A. S. The Theoretical Shape of Sucrose Crystals from Energy Calculations. *J. Cryst. Growth* **1983**, *61*, 546−555.

(18) Hiasa, T.; Sugihara, T.; Kimura, K.; Onishi, H. FM-AFM Imaging of A Commercial Polyethylene Film Immersed in *n*-Dodecane. *J. Phys. Condens. Matter* **2012**, *24*, No. 084011.

(19) Horcas, I.; Fernández, R.; Gómez-Rodríguez, J. M.; Colchero, J.; Gómez-Herrero, J.; Baro, A. M. WSXM: A Software for Scanning Probe Microscopy and a Tool for Nanotechnology. *Rev. Sci. Instrum.* **2007**, *78*, No. 013705.

(20) Momma, K.; Izumi, F. VESTA 3 for three-dimensional visualization of crystal, volumetric and morphology data. *J. Appl. Crystallogr.* **2011**, *44*, 1272−1276.

(21) Beevers, C. A.; McDonald, T. R. R.; Robertson, J. H.; Stern, F. The crystal structure of sucrose. *Acta Cryst* **1952**, *5*, 689−690.

(22) *Handbook of Chemistry: Pure Chemistry*; 4th ed.; Chemical Society of Japan: Maruzen, Tokyo, Japan, 1993; pp II-132−II-133.

(23) Sader, J. E.; Jarvis, S. P. Accurate Formulas for Interaction Force and Energy in Frequency Modulation Force Spectroscopy. *Appl. Phys. Lett.* **2004**, *84*, 1801−1803.

(24) Reischl, B.; Watkins, M.; Foster, A. S. Free Energy Approaches for Modeling Atomic Force Microscopy in Liquids. *J. Chem. Theory Comput.* **2013**, *9*, 600−608.

(25) Amano, K.; Suzuki, K.; Fukuma, T.; Takahashi, O.; Onishi, H. The Relationship between Local Liquid Density and Force Applied on a Tip of Atomic Force Microscope: A Theoretical Analysis for Simple Liquids. *J. Chem. Phys.* **2013**, *139*, 224710.

(26) Suzuki, K.; Oyabu, N.; Kobayashi, K.; Matsushige, K.; Yamada, H. Atomic-resolution imaging of graphite−water interface by frequency modulation atomic force microscopy. *Appl. Phys. Express* **2011**, *4*, 125101.

(27) Söngen, H.; Jaques, Y. M.; Zivanovic, L.; Seibert, S.; Bechstein, R.; Spijker, P.; Onishi, H.; Foster, A. S.; Kühnle, A. Hydration Layers at the Graphite−Water Interface: Attraction or Confinement. *Phys. Rev. B* **2019**, *100*, 205410.
(28) Minato, T.; Araki, Y.; Umeda, K.; Yamanaka, T.; Okazaki, K.; Onishi, H.; Abe, T.; Ogumi, Z. Interface Structure between Tetraglyme and Graphite. *J. Chem. Phys.* **2017**, *147*, 124701.
(29) Hiasa, T.; Kimura, K.; Onishi, H. Cross-Sectional Structure of Liquid 1-Decanol over Graphite. *J. Phys. Chem. C* **2012**, *116*, 26475−26479.
(30) Hiasa, T.; Kimura, K.; Onishi, H. Two-Dimensional Distribution of Liquid Hydrocarbons Facing Alkanethiol Monolayers Visualized by Frequency Modulation Atomic Force Microscopy. *Colloids Surf., A* **2012**, *396*, 203−207.
(31) Fukuma, T.; Ueda, Y.; Yoshioka, S.; Asakawa, H. Atomic-scale distribution of water molecules at the mica-water interface visualized by three-dimensional scanning force microscopy. *Phys. Rev. Lett.* **2010**, *104*, No. 016101.
(32) Kimura, K.; Ido, S.; Oyabu, N.; Kobayashi, K.; Hirata, Y.; Imai, T.; Yamada, H. Visualizing water molecule distribution by atomic force microscopy. *J. Chem. Phys.* **2010**, *132*, 194705.
(33) Hiasa, T.; Kimura, K.; Onishi, H. Hydration of Hydrophilic Thiolate Monolayers Visualized by Atomic Force Microscopy. *Phys. Chem. Chem. Phys.* **2012**, *14*, 8419−8424.

https://dx.doi.org/10.1021/acsomega.9b02660
ACS Omega 2020, 5, 2569−2574